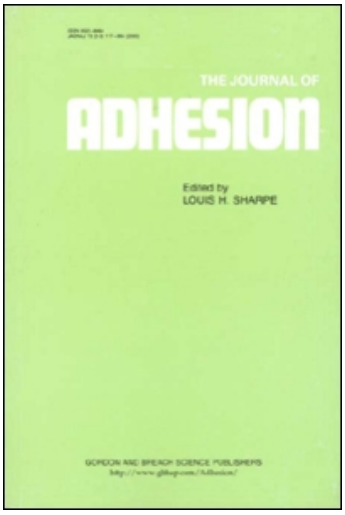

The Journal of Adhesion
Publication details, including instructions for authors and subscription information:
http://www.informaworld.com/smpp/title~content=t713453635

The Interfacial Bond Strength in Glass Fibre-Polyester Resin Composite Systems

J. B. Shortall[a]; H. W. C. Yip[a]
[a] Department of Metallurgy and Materials Science, The University of Liverpool, Liverpool, U.K.

To cite this Article Shortall, J. B. and Yip, H. W. C.(1976) 'The Interfacial Bond Strength in Glass Fibre-Polyester Resin Composite Systems', The Journal of Adhesion, 7: 4, 311 — 332
To link to this Article: DOI: 10.1080/00218467608075062
URL: http://dx.doi.org/10.1080/00218467608075062

J. Adhesion, 1976, Vol. 7, pp. 311–332

Printed in Scotland

The Interfacial Bond Strength in Glass Fibre-Polyester Resin Composite Systems

Part I. The Measurement of Bond Strength

J. B. SHORTALL and H. W. C. YIP

Department of Metallurgy and Materials Science, The University of Liverpool, P.O. Box 147, Liverpool, U.K.

(*Received June 5, 1975*)

The interfacial bond strength in glass fibre–polyester resin composites has been investigated using various experimental techniques. These included blocks of resin containing fibre (in which, depending on the geometry of the specimen, failure occurs in either a shear or tensile mode) the pullout of a fibre from a disc of resin and a short beam shear test for interlaminar shear strength determination.

Low power optical microscopy and optical retardation measurements of stress induced birefringence were used to detect the difference between intact and debonded fibre resin interfaces. The shear modulus and shear strength of the resin were obtained from torsion tests on cylindrical rods of the resin.

The single fibre shear debonding specimen and the short beam shear test are shown to be the most viable test methods but interpretation of the results is complicated by the various modes of failure possible and by the different stress states which exist in the area of the specimen where debonding starts. Stress concentration factors obtained by finite element analysis and photoelastic analysis have been applied to the results from these tests and the corrected interfacial bond strengths are in close agreement.

The real interfacial bond strengths of well bonded glass-fibre polyester resin systems is shown to be of the order of 70 MN m^{-2}.

I. INTRODUCTION

The interfacial bond strength in glass fibre–polyester resin composites is of fundamental importance through its significant effect on the ultimate properties and the failure behaviour of these materials. It is, however, an elusive quantity for several reasons. Like other material strengths, it is

subject to statistical variation with regard to flaw and impurity distribution, etc. Also, the molecular structure of the fibre–resin interface region is complex and there is a corresponding lack of quantitative explanation for the mechanism and quality of the interfacial adhesive bond. Furthermore, the criterion for interfacial fracture is not well understood and this renders the exact analysis of the failure mode difficult.

There has been a lack of systematic investigation into the interfacial bond strength of composite systems although, over the past decade, various methods have been employed to measure this property; methods which have not always given consistent results. Also, the effect of processing variables on interfacial bond strength has received little attention. Consequently, there is a need to fill the gap which exists between the gross failure behaviour and the local response and between the average strength and its molecular interpretation.

An extensive investigation, the first part of which is reported here, has been carried out to evaluate the various experimental methods available for measuring bond strength and to show the true magnitude of interfacial bond strength in glass fibre–polyester resin systems. Also, in order to estimate the real strength of the interfacial bond, a knowledge of the interfacial stress distribution is necessary. Although several theoretical models have been proposed,[1-6] all predicting high shear stress concentrations near the fibre end regions the practical approach is to apply the results from photoelastic analysis[7,8] (both two-dimensional and three-dimensional) and finite element analysis[9-11] (two-dimensional) of a composite model.

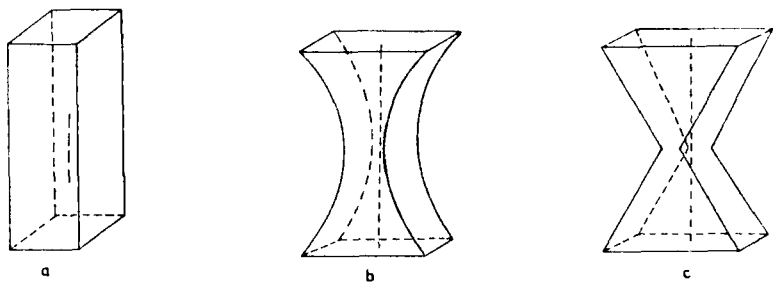

FIGURE 1 Single fibre specimens: (a) Rectangular, (b) curved neck, (c) trapesoidal.

A number of experimental methods are available for the measurement of bond strength. The first method involves the use of a single filament, discontinuous or continuous embedded in a matrix, the dimensions of which greatly exceed those of the fibre; the three possible geometrical arrangements for single filament specimens are shown in Figure 1. Figure 1(a) shows a rectangular block of matrix containing a discontinuous fibre. Under uniaxial

compression, failure will initiate near fibre end regions as predicted theoretically.[12] Figure 1(b) shows the curved neck specimen which has been employed extensively for the measurement of interfacial bond strength.[12] When such a specimen is compressed in the fibre direction and assuming elastic behaviour of the system, the difference in the Poisson's ratios of the two materials gives rise to an interfacial tensile debonding stress in the radial direction. Figure 1(c) shows a double trapezoidal specimen. The sharply sloping faces produce a shear stress when the specimen is subject to compression along the fibre axis.[13]

The second method of measuring interfacial bond strength involves the use of a real composite containing a significant percentage of reinforcing fibre. These fibres, when staying in close proximity may interact, thus resulting in a stress state different from that of an isolated fibre embedded in an infinite resin matrix. There is therefore a need to study the effect of the presence of neighbouring fibres. This is done conveniently by means of the short beam shear test on composite beams of different fibre volume fractions.[14] Figure 2 shows the short beam shear specimen geometry.

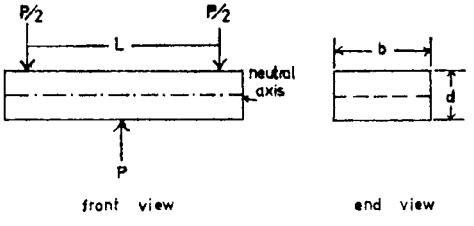

FIGURE 2 Short beam shear specimen.

In the presence of complicated modes of failure, the use of the results of classical beam theory is inappropriate and, although it is possible to determine the lower bound of the shear strength, it would appear more beneficial to use a torsion test on composite specimens, in which case only shear forces are present and the results are easier to interpret.[15] An additional test method involves the pull out of a rod from a disc of resin which is cast on a non-adhesive surface.[16,17] In order for the test to be successful weak interfacial bonding is a prerequisite in which case a large embedded length can be used, thus rendering unimportant the wetting of the fibres by capillary action.

2. EXPERIMENTAL

2.1. Materials

Two unsaturated polyester resins were employed in the investigation. The filabond 8000 resin manufactured by Synthetic Resins Ltd. is a hot curing resin with medium reactivity, cross-linked by styrene. The catalyst is MEK

peroxide and the accelerator is cobalt naphthenate. The Crystic 195 resin is manufactured by the Scott Bader Company Ltd. Methyl methacrylate is the coreactive solvent and the catalyst and accelerator are the same as those used in the Filabond 8000 resin system. The resin types are summarized in Table I.

TABLE I

Polyester resins

Trade name	Manufacturer	Parent compound	Coreactive solvents	Curing conditions	Catalyst and accelerator
Crystic 195	Scott Bader Co. Ltd.	Maleic and phthalic anhydride, propylene glycol	Methyl metha-crylate	Room tempera-ture	M(MEK peroxide) E(Cobalt Napthenate)
Filabond 8000	Synthetic Resin Ltd.	Unknown	Styrene	Hot 120°C 5 hours	K(MEK peroxide) E(Cobalt Napthenate)

The E-glass fibres used were supplied by the Pilkington Research and Development Laboratories in the form of rovings with a nominal diameter of 30 μm; the usual 13 μm fibres were too difficult to manipulate in the single filament specimen preparations. Water spray had been applied to the rovings to protect them against abrasive damage but, otherwise, the fibres were regarded as "untreated" in the as received form.

The surface treatments used in the initial evaluation of test methods comprised γ-methacryloxypropyltrimethoxy silane (a silane coupling agent reactive towards both the glass and the polyester resin), tetradecyl pyridinium bromide, a boundary lubricant, and polyvinyl acetate, a film forming polymer which is used to promote adhesion between filaments. The fibres were heat cleaned at 500°C for 2 hours to remove weakly adsorbed low molecular weight substances and the surface treatment then applied in the form of an aqueous solution, the pH of which was brought to the range 3.5–4.0 by means of a buffer solution. The treated fibres were then dried at 113°C for 2 hours under atmospheric pressure.

2.2. Specimen preparation

The single fibre specimens illustrated in Figures 1(a)–1(c) were cast in steel moulds from which up to twenty specimens could be obtained in a single casting. However, only a small fraction were of sufficiently good quality (in terms of dimensional accuracy, fibre alignment and consistency in residual

stress distribution) to be chosen for testing. The casting was a two stage process, half of the resin being poured into the mould, the fibres laid in place before gelation occurred and the second half of the resin then poured on top.

The specimen dimensions chosen were $10 \times 10 \times 30$ mm with a fibre length of 10 mm. This geometry was chosen to avoid the buckling of the resin column at the stress at which interfacial failure occurs (determined by theoretical analysis) and fibre buckling (determined by microscopic examination). Slenderness ratio values were obtained using the analysis for the critical buckling stress of a rectangular column.[18] A value of 3 (recommended for compression tests in general[19]) was obtained. These dimensions prevented the end constraint effects exerting any serious influence on the stress states near the fibre ends.

The curved neck specimens used had a radius of curvature of 20 mm and a height of 30 mm. The trapezoidal specimens had a height of 30 mm and the sides subtended an angle of 60° with the top and bottom surfaces.

The short beam shear test specimens were prepared in a dual channel leaky mould; prewetted fibre bundles were placed in the channels and a plunger applied slowly, with the aid of a hydraulic press, to squeeze out the excess resin and entrapped air. The specimens used had dimensions of $24 \times 8 \times 4$ mm. This allowed an overhang of 2 mm which has been shown to have no effect on test results.[14]

The pull out test specimen was cast on a specially designed test fixture which provided facilities for gripping the glass fibre (either as a bundle or a rod) indirectly through a resin block.

The cast specimens were cut to the dimensions required using a low speed diamond saw. They were then examined with a low power stereomicroscope to detect any fibre prominence resulting from inadequate bonding.

Following this, they were viewed between crossed polars and only those specimens with similar isochromatic patterns were used. Finally, the top and bottom surfaces were made parallel by polishing in a specially designed polishing jig and the straight sides from the saw cut were kept perpendicular to the top surface by polishing in a similar way.

2.3. Mechanical testing and monitoring of interfacial failure

The single fibre specimens were tested in uniaxial compression in the fibre direction using an Instron testing machine. Debonding and subsequent damage was followed optically by either a low power microscope or the naked eye under lighting conditions which approached those of dark ground illumination. Only static loading was applied with a cross head speed of 0.2 mm/min. In order to reduce the end constraints due to friction, a thin layer of molybdenum disulphide dust dispersed in a silicone resin was applied to the top and bottom surfaces for lubrication.

The short beam shear test was performed using a three-point bend rig[14] which allowed the L/D to vary from about 3 to 15 at a beam depth of 4 mm. The loading noses had a radius curvature of 3.2 mm which is within the range recommended in the ASTM specifications.[20] The bend rig was used in conjunction with an Instron machine. A Zeiss Tessovar photomicrographic recording system was fixed to the Instron machine so that the top and front views of the specimen could be photographed from different angles without difficulty. Throughout the whole investigation, the L/D ratio was chosen to be 5.5 and V_f equalled 0.45. These conditions gave shear failure and showed little compressive damage at the contact point between the specimen and the central loading nose. The cross head speed was fixed at 0.2 mm/min.

The pull-out test was performed on a loading rig which allowed indirect gripping of the fibres and tensile loading to be applied to the resin disc. Full details are given elsewhere.[21] The cross head speed used was 0.5 mm/min.

2.4. Optical retardation measurements

Polyester resin shrinks during the curing process and hence the composite formed by transparent resin and discontinuous fibre will exhibit optical birefringence. Stress induced birefringence accounts for the major part of the overall birefringence while the molecular orientation of resin makes a small contribution.

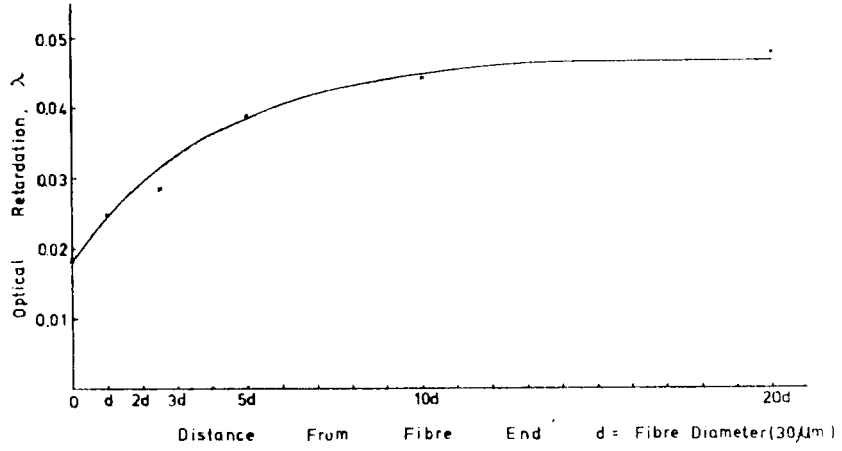

FIGURE 3 Variation of retardation with distance from fibre end.

For an interface which is incapable of supporting any shear stress, there can be no build-up of axial fibre stress along the fibre. Consequently there should be no variation of optical retardation along the fibre, assuming that the contribution to birefringence resulting from plastic strains in the resin is negligible.

Optical retardation measurements were carried out to examine the difference between an intact and a debonded fibre-matrix interface. The thin film used was of the order of 200 μm in thickness and contained a completely embedded fibre. The debonded interface was cut from a debonded rectangular specimen. Figure 3 shows the variation of optical retardation with distance from the fibre end of a specimen which had been deformed to the point just before the onset of threshold debonding. No such variation of optical retardation with distance was obtained from a debonded interface.

The measurements were made using a Cooke elliptic compensator in conjunction with a Reichert Zetopan polarizing microscope.

3. RESULTS

3.1. Shear debonding rectangular specimens with discontinuous fibre

These specimens using Filabond 8000 resin showed several stages of interfacial failure. The first stage of failure occurred near the fibre ends, where the stress concentrations were the highest, at an average stress of 38 MN m^{-2}. This was often overlooked by the naked eye as the debonded length was only of the order of 100 μm (Figure 4(a)). Thin slices, cut from the specimen when it had been stressed to a level immediately before the onset of debonding, showed that the variation of optical retardation with distance from the fibre end agreed well with that which an intact fibre–resin interface would produce as a result of stresses due to resin shrinkage. The second stage of failure involved the formation of stable cracks which were of the order of 1.5 mm long and clearly visible (Figure 4(b)). The mean value of the stresses needed to form these cracks, which had different values due to the differences in fibre end geometry, was designated σ_s. The third stage of failure was the rapid propagation of the interfacial cracks towards the centre of the specimen, Figure 4(c), at a mean stress level of σ_p. Lastly, the whole fibre underwent debonding.

A small number of rectangular specimens were made using the crystic resin and 500 μm diameter glass rods which were surface treated in a similar way to the 30 μm fibres. These specimens showed signs of debonding near the fibre end region before testing; otherwise the value of σ_s obtained (>23.3 MN m^{-2}) was much lower than the corresponding value of σ_s using the 30 μm fibres.

A situation intermediate between the single fibre model and one with a high volume fraction of fibre as far as possible fibre interaction is concerned is that involving the use of a bundle of discontinuous fibres. Small bundles containing up to one hundred fibres were used in place of a single filament in the rectangular type specimen. The initial stage of debonding was similar to the single filament case, i.e. interfacial separation started near the two fibre

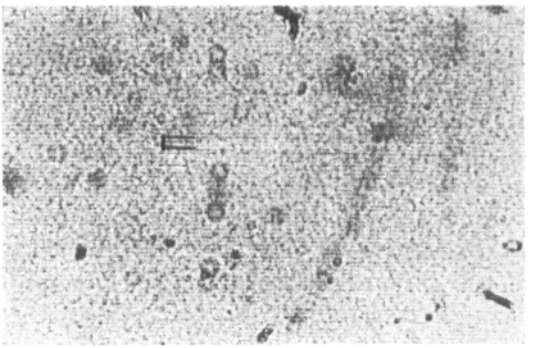

a

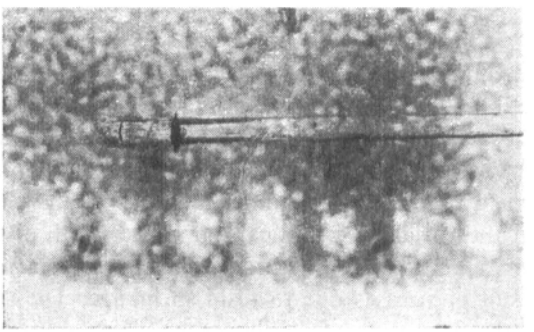

b

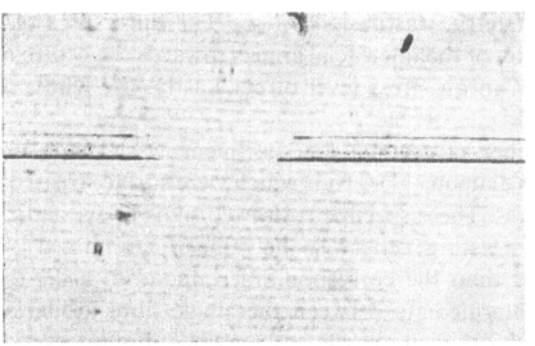

c

FIGURE 4 Interfacial debonding in rectangular specimens (optical microscope). (a) First stage, (b) formation of stable cracks, (c) propagation of cracks towards the centre of the specimen.

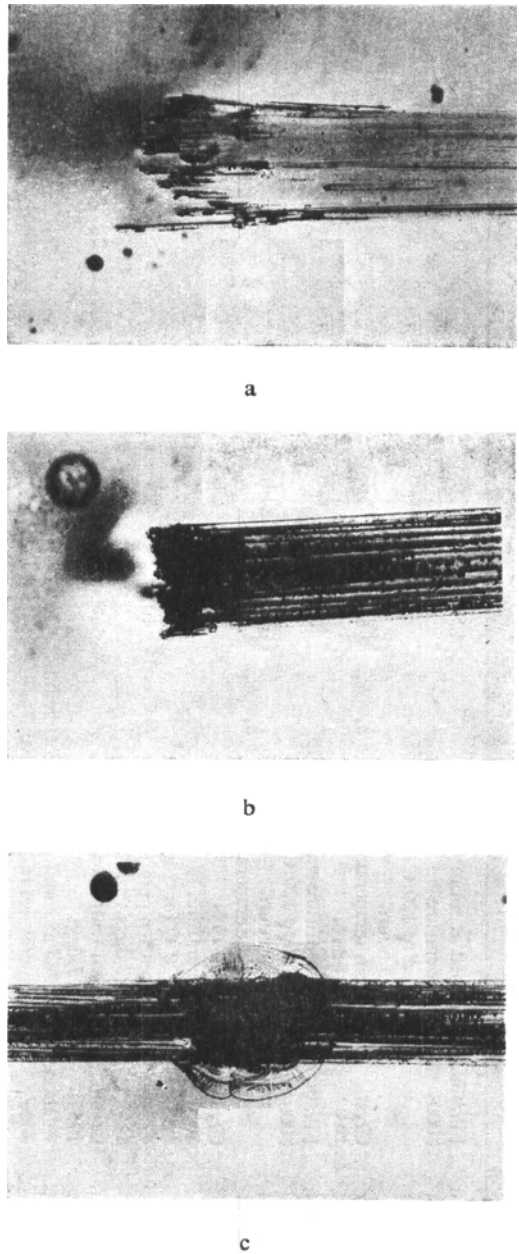

FIGURE 5 Stages of debonding and subsequent damage in a rectangular specimen containing a small number of fibres (Optical Microscope): (a) Onset of debonding near the end of a fibre bundle, (b) extension of cracks, (c) debonding and matrix failure.

TABLE II

Relative order of interfacial bond strength using different resins and different specimen geometry

Specimen geometry	Resin	Curing condition	Quantity measured	Mean value MN m^{-2}	Coefficient of variation	Range	No. of specimens tested	Remarks
Rectangular	Filabond 8000	Gelled at room temperature raised to 120°C for 5 hours	σ_s	52.8	20.6	38.2	10	
Rectangular	Crystic 195	Room temperature for 7 days	σ_s	60.5	14.8	34.7	25	
Rectangular (glass rods)	Crystic 195	Room temperature for 7 days	σ_s	>23.3			5	
Rectangular (fibre bundles)	Crystic 195	Room temperature for 7 days	σ_s	38–60.5				
Curved neck	Filabond 8000	Gelled at room temperature, raised to 120°C for 5 hours	τ_t	>11.2	9.3		6	Debonding occurred in plastic region
Curved neck	Crystic 195	Room temperature for 7 days	τ_t	>10.2			5	Debonding occurred in plastic region
Trapezoidal	Crystic 195	Room temperature for 7 days	τ	>6	—	—	2	Debonding occurred in plastic region
Short beam shear	Filabond 8000	Gelled at room temperature, raised to 120°C for 5 hours	Short beam shear strength	56.7	9.7	7.1	5	
Short beam shear	Crystic 195	Room temperature for 7 days	Short beam shear strength	>39.7	1.7	1.7	5	Yielding of short beam
Pull out (glass rod)	Crystic 195	Room temperature for 7 days	τ	>23.3	—	—	5	Breakage of glass rod

end regions. The propagation of this crack sometimes did not start from the cracked interface but at a site with the highest stress concentration. This is not surprising as there was considerable difficulty in getting the inner fibres completely wetted by resin. A small number of specimens showed that the threshold debonding stress and σ_s all fell within the range of values reported in the single filament case, i.e. 38 to 60.5 MN m^{-2}. Figure 5(a), (b) and (c), shows the stages of debonding and subsequent damage to the composite in the multi-filament case.

Measured interfacial bond strength using both resins and single fibres, bundles and rods are given in Table II.

3.2. Tensile debonding curved neck specimens with continuous fibre

Failure occurred in the middle of the specimens where the cross-sectional area was smallest and the tensile debonding stress at its maximum. In some cases discontinuous debonding was observed (Figure 6) which may have resulted from the fibre buckling. No debonding or fibre failure was observed in the elastic region of the stress–strain curve. Failure did occur in the plastic region and this would warrant some modification of the stress criterion for the failure of brittle materials. In practice there is considerable difficulty in obtaining an accurate measurement of the plastic strain and hence the use of the curve neck specimens could not give as straightforward a failure criterion as the rectangular type specimen does. The measured bond strengths with this specimen geometry are given in Table II.

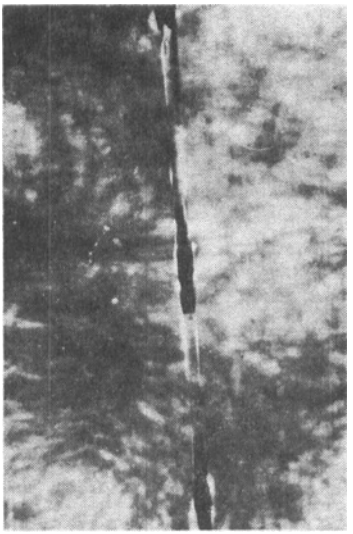

FIGURE 6 Discontinuous debonding in a curved neck specimen.

3.3. Double trapesoidal specimens with continuous fibre

In this specimen failure again occurred in the plastic region of the stress–strain curve. The lower bound of the shear debonding stress was found to be 6 MN m^{-2}. Similar reservations against the use of this specimen apply as in the case of the curved neck specimen. A further drawback of the geometrical configuration is that the stress on the plane of minimum cross-section varies from a maximum at the edge to a minimum at the centre in an abrupt manner. When 30 μm thin fibres were used it was difficult to keep them strictly in the middle. Hence the stress around the fibre where debonding or fibre failure was expected to occur varied considerably from one specimen to the other and raised further doubts concerning the viability of this method. The measured bond strength is given in Table II.

3.4. Short beam shear test

The failure mode in the short beam shear test depends to a large extent on the strength properties of the resin. With a high strength resin such as the

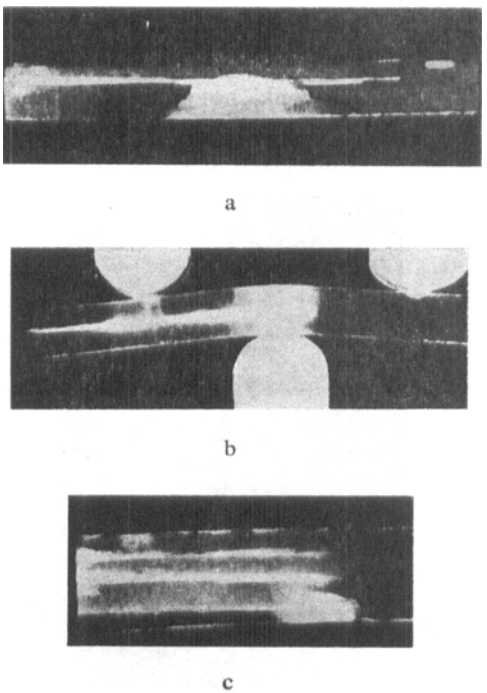

FIGURE 7 Shear failure of a composite beam (Tessovar Photomicrographs): (a) Failed specimen, (b) onset of failure in a test run, (c) multiple shear failure planes.

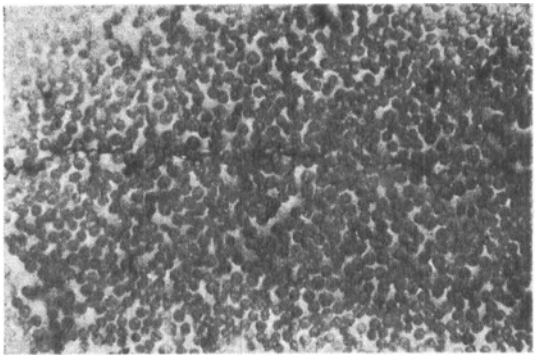

FIGURE 8 Transverse section photomicrograph of a failed composite beam.

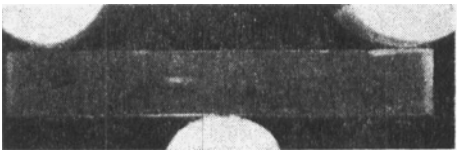

Stage 1

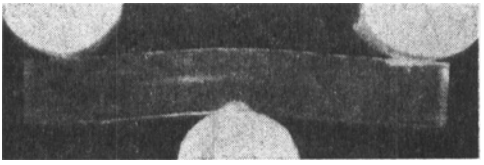

Stage 2

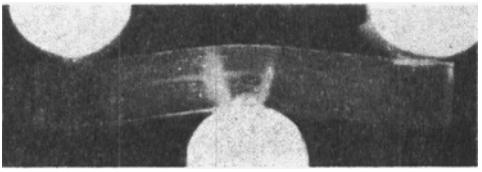

Stage 3

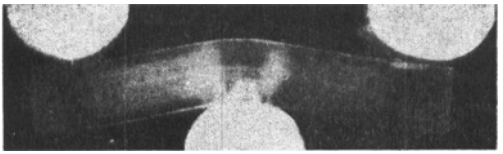

Stage 4

FIGURE 9 Short beam shear test with yielding: different stages of damage development.

Filabond 8000 shear failure was obtained when L/D was below about 5 and V_f was 0.45. Figure 7(a) shows a failed composite beam and 7(b) shows the same specimen in the presence of the loading noses in a test run. The load deflection curve showed a sharp fall and if deformation was allowed to continue, multiple shear planes would develop (Figure 7(c)) and correspond to a lower peak in the load deflection curve. The failure plane as shown in Figure 8 was not strictly horizontal.

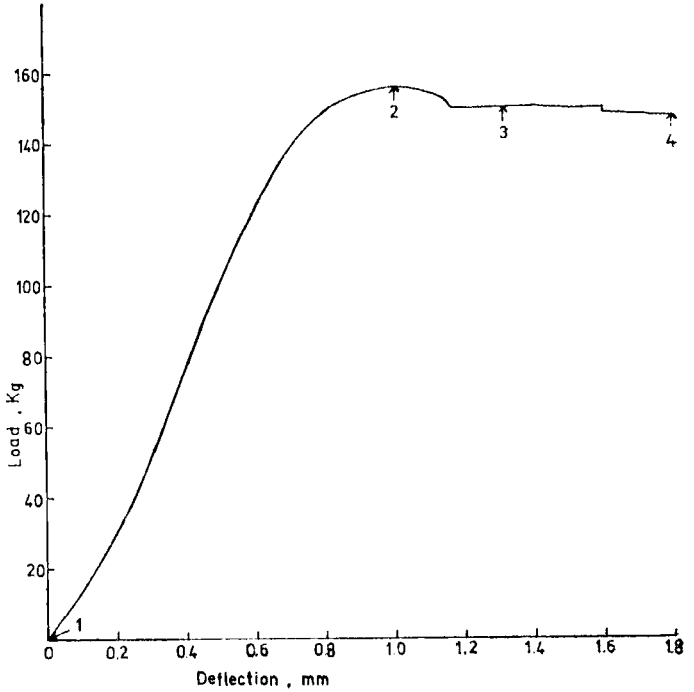

FIGURE 10 Load-deflection curve for short beam shear specimen.

If the composite beam showed yielding before shear failure, as was the case with the Crystic 195 resin, specimen damage appeared to start near the central loading nose where the shear stress concentration was at its highest. This was accompanied by white loops of yielded regions radiating outwards from the central loading nose. A clear failure plane did not usually develop. The stages of damage are shown in Figure 9 and the corresponding load deflection curve is shown in Figure 10. The short beam shear test results are listed in Table II.

3.5. Fibre pull-out test

Three modes of failure were observed when a bundle of fibres was used. If the interfacial bond was strong, if the embedded length was large or if

there was a flawed fibre, the fibre failed in tension. This happened with a relatively thick resin disc (about 1 mm in thickness) which gave rise to tensile failure of a small fraction of the fibres plus some fibre pull-out leaving a few small holes on the resin disc. Figure 11(a) shows the thick resin disc with the holes and some fibres left behind.

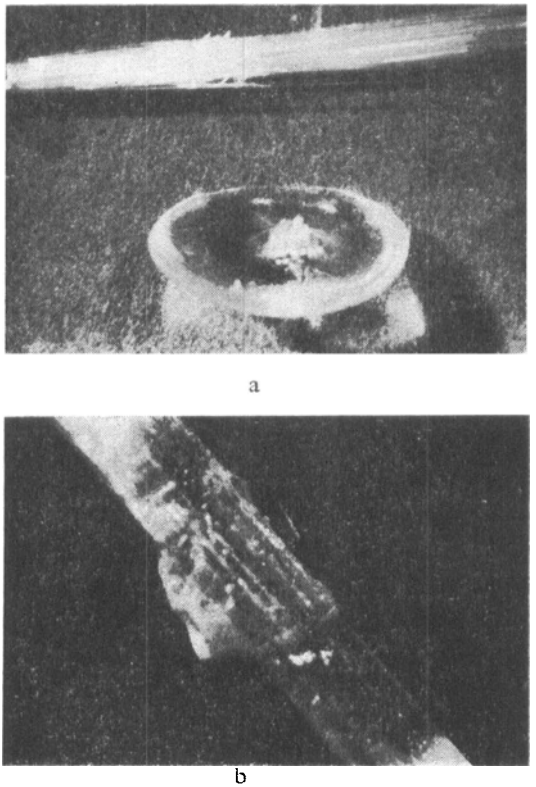

a

b

FIGURE 11 Pull-out test (Optical Micrographs): (a) Resin disc with holes and some fibre remaining, (b) pulled out fibre bundle carrying resin.

A second mode of failure usually occurred when the resin disc was relatively thin (in the region of 0.1 mm or less), in which case the stiffness of the disc could not support the excessive bending and thus failed cohesively. Such a case is illustrated in Figure 11(b) which shows the pulled out fibre bundle carrying a significant amount of resin.

It was difficult to estimate the interfacial area between the fibre and the resin and hence the calculation of the interfacial shear strength was not likely to be accurate. Resin discs of intermediate (0.1 to 1 mm) and controllable thickness were difficult to obtain in practice.

Genuine, clean fibre pull out was never obtained. The breakage invariably started somewhere below the top of the resin core (formed as a result of wetting) reached the interface and followed the fibre direction until debonding was completed.

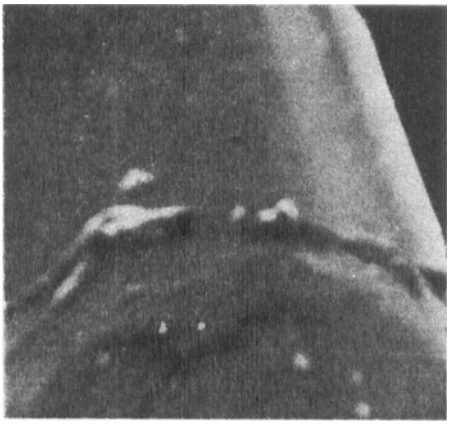

FIGURE 12 Scanning electron micrograph of portion of pulled out glass rod.

Because of the complexity of the failure mode and the difficulty in controlling the embedded length 500 μm E-glass rods were used instead of fibre bundles. When a pull out was successful (without fibre failure) the resin disc was sectioned and examined microscopically. The embedded length was then measured and the interfacial shear strength calculated assuming a constant value of τ. The results were much lower than those from the short beam shear test or single filament shear debonding test (Table II).

Figure 12 is a scanning electron micrograph of a pulled out rod at the breaking point of the resin sheath.

3.6. Shear properties of polyester resins

A knowledge of the shear modulus and shear strength of the resins was necessary for the interpretation of experimental results. These were obtained

TABLE 3

Shear properties of cured polyester resin

Resin	Curing condition	Shear strength MN m^{-2}	Shear modulus GN m^{-2}
Filabond 8000	120°C, 5 hours	64.4	1.58
Crystic 195	Room temperature 6 weeks	60.7	1.24

from the torsion test on cylindrical rods of resin samples and are given in Table III. The values obtained are very close to those predicted by theory.

4. DISCUSSION

4.1. Order of magnitude of bond strength and discrepancy between test methods

Table II summarizes the relative order of bond strengths using the different resins and different specimen geometries. The results from the various test methods indicate that the interfacial bond strength between the treated glass fibres and polyester resin is approaching the cohesive strength of the resin. This is several times higher than the figures reported earlier[22] which were of the order of 10 MN m^{-2}. Failure was not cohesive, as is confirmed by the clean interfacial gap, seen in Figure 4, which shows the contrast between the debonded interface (dark) and intact (bright) interface.

The apparent strengths vary amongst the different methods with the pull out test yielding approximately one third of the values obtained from the single filament shear debonding and the short beam shear tests. The latter two tests gave results of the same order of magnitude except where specimen yielding occurred.

However, even making allowance for experimental error, the discrepancies between the methods must be accounted for in terms of:

a) The difference in the stress states in the specimen prior to testing (due to the different residual stresses introduced during processing) and due to external loading (since these specimens have different symmetry).

b) The difference in stress concentration: whether the fibre is continuous or discontinuous, fibre end geometry in the case of discontinuous fibres, fibre interaction in the case of high V_f composites, void content, void size and distribution at the interface, fibre to resin modular ratio.

c) The difference in the failure mode: adhesive (interfacial) failure or cohesive (resin) failure, brittle failure or resin yielding.

d) The surface topography and molecular structure of the glass rod, when results are to be compared with those obtained from much smaller, 30 μm fibres.

The factors mentioned above have to be considered in order to achieve a better understanding of the strength and failure of glass fibre–polyester resin interfacial bonding in either qualitative and semi-quantitative terms.

4.2. Real interfacial bond strength

Material heterogeneity together with geometrical discontinuities present in the fibre–resin composite give rise to stress concentrations which raise the local stresses to values above the σ_s and short beam shear strengths listed in Table II.

The maximum stress concentration factor at the end of a single fibre in a resin is about 2.[7] Since the onset of debonding occurred at 38 MN m^{-2} in the case of the shear debonding single fibre specimens using Filabond 8000 resin the local stress at failure would be about twice this value, i.e. of the same order of magnitude as the shear failure stress of the pure resin. Theoretical analysis predicts that such a system would exhibit both cohesive and adhesive modes of failure.[23] However, because of the difficulty in recording the stress at the onset of initial debonding the stress at which this debonded area developed into a stable interfacial crack was recorded as σ_s. Since the interface has debonded prior to σ_s, the magnitude of this quantity will not be strongly dependent on largely uncontrollable factors such as fibre end geometry and one would expect it to depend largely on the chemical and mechanical bonding which keeps the interface intact. The stress intensity of such a cracked interface can be treated to a first approximation by a two-dimensional finite element model which permits the calculation of the elastic stress intensity factor associated with stress fields near a partially debonded interface (the interfacial stress intensity factor).[24] By this means numerical solution of the interfacial stress intensity factor, K_2, was obtained as a function of crack length using the expression[24]

$$K_i = \frac{K_2\sqrt{w}}{\mu_0 G_1}$$

where K_i is obtained from appropriate tables, w is the length of the interface, G_1 is the shear modulus of the resin and μ_0 is the matrix displacement obtained from the appropriate stress–strain curve.

With the shear moduli obtained from the torsion test (Table III) the matrix displacement obtained from the stress–strain curve and the crack length measured with the microscope (of the order of 1.5 mm) K_2 is found to have a value of 1.35. This is very close to the stress concentration factor of approximately 1.30 suggested by other workers for a short beam shear specimen containing 45% carbon fibre in an epoxy matrix.[15]

If the values of σ_s are multiplied by 1.35 the products are somewhat in excess of the shear strength of the pure resin (64.4). There are three possible explanations for this. Firstly the interfacial material may show plastic yielding in compression similar to that of the resin. The plastic deformation at the crack tip blunts the crack and thus the local stress does not exceed the yield stress of the matrix in the bulk. Another possibility is that the resin in the immediate vicinity of the reinforcing fibres has undergone some significant change in mechanical behaviour (e.g. modulus, shear failure stress, T_g) as a result of the structural changes (at the molecular level) brought about by the special nature of the fibre–resin interaction (high surface to volume ratio) which is by no means the same as the interaction of the same materials in the

bulk. Lastly the two-dimensional fracture mechanics model so far used is only approximate and a more realistic one to represent the real composite will necessarily be three-dimensional.

An important result from the partially debonded laminate model is that K_2 is rapid at first but appears to approach some limiting value asymptotically. The implication is that whenever the reinforcing fibre breaks and debonding occurs around the fractured ends the interfacial cracks are self-arresting. In other words for a given crack length the load would have to be raised to increase the interfacial stress intensity factor. This explains the difference in the values of σ_s and σ_p in the single fibre rectangular type specimens.

The main reason for the widespread use of the short beam shear test is its simplicity in specimen preparation and mechanical testing. When the mode of failure is shear and in the absence of any significant compressive damage (at the point of contact between the specimen and the loading nose) and of tensile failure on the opposite side of the specimen the test is at least valid as a qualitative method of comparison. However, with the use of fracture mechanics, it is possible to calculate the theoretical stress concentration factor due to the inhomogeneity of material for a system with known fibre to resin shear modulus ratio and V_f. The value of this stress concentration factor is approximately 1.30[15] for a system which corresponds to those 45% fibre specimens tested in the present investigation. This effectively means that the true short beam shear strength (Table II) is above the shear strength of the pure resin.

Using the appropriate stress concentration factors the results from the shear debonding specimen test and the short beam shear test can be shown to be very similar and are listed in Table IV.

TABLE IV

Real interfacial bond strengths, MN m^{-2}
Resin: Filabond 8000

Test specimen	Measured bond strength	Stress concentration factor	Real bond strength
Shear debonding rectangular specimens	$\sigma_s = 52.8$	1.35	71.3
Short beam shear test	$\tau = 56.7$	1.30	73.7

The yielding behaviour of composites using the Crystic 195 resin requires a different treatment. The yielding of short beams at failure requires a reassessment of the shear stress distribution of the orthotropic elastic–plastic short beam along its depth. Recently, this problem has been studied by means of

two-dimensional finite element analysis. The results indicate that classical estimates of maximum shear stress underestimate this quantity by as much as 100%.[11] Furthermore, classical treatment does not give an assessment of the conditions of combined stress which are critical in the vicinity of the loading nose where debonding and fracture occur. In the Crystic 195 composite specimens no buckling of the fibres was observed and the modes of failure are confined to shear debonding and indentation at the loading nose. Increasing the apparent short beam shear strength by 100% will give values of approximately the same order as those for Filabond 8000 resin when the corresponding stress concentration factor is taken into account, i.e. a value of 79.4 MN m^{-2} for the Crystic 195 compared with a value of 73.7 MN m^{-2} for the Filabond 8000. Furthermore, if the stress concentration factor obtained from the single fibre test (1.35) is applied to σ_s for the Crystic 195 a bond strength of 81.6 MN m^{-2} is obtained which compares favourably with the estimated value above. Although local yielding presumably occurred in the Crystic 195 single fibre shear debonding specimen, the presence of only one filament means that, unlike the short beam shear specimen which contains a high volume fraction of fibres, the bulk of the resin in the sample still remains elastic at σ_s.

The pull out test gave the lower bound of the interfacial shear strength, Table II. Some possible explanations are as follows:

a) The surface profile of the resin disc near the rod/resin junction has so far been neglected. The wetting of the glass rod by the polyester resin gives rise to the curving up of the top and bottom surface of the resin disc. This may be considered as the lower half of an (imaginary) elliptical crack in contact with the glass rod. The stress concentration facilitates failure when the disc is under tensile loading.

b) The surface of the crude E-glass rod has not been well-characterized and it is possible that the surface characteristics are different from those of the much smaller 30 μm fibres in terms of, for example, the number of active sites available per unit area of the glass surface.

c) The residual stresses produced in the pull-out specimen due to resin curing are different from those in the other types of specimens. However, in view of the relatively minor role played by the residual stresses in the overall bonding this alone cannot account for the difference in the behaviour of the rod and the fibres.

d) The calculation leading to the interfacial shear strength assumes a uniform shear stress along the length of the embedded fibre as a first approximation to pull-out from an elastic matrix. However, it has been pointed out that calculated values of the interfacial shear strengths are likely to be low.[16,17]

CONCLUSIONS

The real interfacial shear strength (i.e. local shear stress at failure) of a well bonded glass fibre polyester composite is of the order of 70 MN m^{-2} and is considerably higher than the figures for apparent interfacial bond strength previously reported.

Of the experimental methods available for measuring the shear strength of the glass fibre polyester resin interfacial bond only two methods appear viable over a wide range of conditions: the single fibre shear debonding specimen and the short beam shear specimen. Even so, the interpretation of the results is complicated by the different modes of failure and the different stress state in the area where debonding starts. The tensile debonding curved neck specimens failed to measure the true debonding values in the systems examined and are limited by yielding in the necked down region.

The true interfacial bond strength can be obtained by estimating the stress concentration factor involved. In the case of the single filament shear debonding test, this was obtained from two-dimensional finite element and photoelastic analysis.

For the short beam shear test the value of the stress concentration factor was obtained from fracture mechanics results given in the literature.

These two factors are numerically close to each other. Also, the apparent bond strength obtained from the single fibre shear debonding test and the short beam shear test agree very well provided that no appreciable plastic yielding occurs before failure.

In the event of yielding of the short beam shear test, results from finite element analysis on an elastic plastic beam, taken from the literature, can be applied to account for the drop in the apparent short beam shear strength. Semi-quantitative results are not obtainable for direct comparison and such results can only be obtained from the torsion test on cylindrical rods of fibre–resin composite specimens.

It is therefore suggested that for the measurement of interfacial shear strength of a glass fibre–polyester resin system the short beam shear test is used first to determine the order of magnitude of shear strength, as this is the quickest of all the tests available. If the apparent short beam shear strength is far below the shear strength of the matrix and no significant yielding occurs before shear failure of the short beam (when no other mode of failure is operative) then the product of the apparent short beam shear strength and the stress concentration factor can be taken as the real shear strength.

If the apparent shear strength found from the short beam shear test is comparable with the shear strength of the cured resin then the single fibre shear debonding specimen and the torsion test must be used instead. The single fibre shear debonding specimen is useful since it is possible to visually observe debonding and record the process.

The torsion test of cylindrical rods of composite specimens in the only method in which no stresses other than shear are present in the composite and this test is needed if accurate results of shear strength are required. In this case specimen preparation difficulties and the sophisticated apparatus required can be a major drawback to the use of the test.

The pull-out test can be used for composite systems of low interfacial strength (below about 10 MN m^{-2}) although some refinement leading to the calculation of the real shear strength of the interface is necessary.

Acknowledgements

The authors wish to express their gratitude to Pilkington Brothers Research and Development Limited for the award of a research studentship (H. W. C. Y.) and to Dr. N. L. Hancox of the Atomic Energy Research Establishment, Harwell, who carried out the torsion experiments.

References

1. H. L. Cox, *Brit. J. Appl. Phys.* **3,** 72 (1952).
2. N. F. Dow, G.E.C. Report R63 SD 61 (1963).
3. B. W. Rosen, *Fibre Composite Materials* Chap. 3. ASM Publication (1965).
4. J. O. Outwater, *Modern Plastics* **33,** 156 (1956).
5. A. Kelly and W. R. Tyson, *J. Mech. Phys. Solids* **13,** 329 (1965).
6. M. R. Piggott, *J. Mat. Sci.* **5,** 669 (1970).
7. J. M. Allison and L. C. Holloway, *Brit. J. Appl. Phys.* **18,** 979 (1967).
8. J. E. Hill, Ph.D. Thesis, Cornell University (1967).
9. A. S. Carrara and F. J. McGarry, *J. Comp. Mat.* **2,** 222 (1968).
10. D. R. J. Owen, J. Holbeche and O. C. Zienkiewicz, *Fibre Sci. and Technol.* **2,** 185 (1969).
11. C. A. Berg, Tirosh and M. Israeili, ASTM STP 460 (1972).
12. L. J. Broutman and F. J. McGarry, MIT Plastics Research Progress Report, Aug. 15 (1961).
13. R. D. Mooney and F. J. McGarry, SPI 14th Am. Reinf. Plast. Conf. Preprints Sec. 12-E (1959).
14. A. W. Christiansen, J. Lilley and J. B. Shortall, *Fibre Sci. and Technol.* **7,** 1 (1974).
15. W. N. Reynolds and N. L. Hancox, *J. Phys. D.* **4,** 1747 (1971).
16. R. C. De Vekey and F. J. Majumdar, *Magazine Concr. Res.* **20,** 229 (1968).
17. P. Lawrence, *J. Mat. Sci.* **7,** 1 (1972).
18. S. P. Timoshenko, *Strength of Materials, 3rd Ed.* (Van Nostrand, 1956).
19. A. S. T. M. E9-52T.
20. A.S.T.M. D 2344-G7.
21. H. W. C. Yip, Ph.D. Thesis, Liverpool University, 1973.
22. L. J. Broutman, *Poly. Eng. & Sci.* **6,** 263 (1966).
23. J. Cook and J. E. Gordon, *Proc. Roy. Soc.* **282A,** 1391 (1964).
24. S. G. Sawyer and R. B. Anderson, *Engr. Fracture Mechanics* **4,** 605 (1972).